Available online at www.sciencedirect.com

ScienceDirect

Physics Procedia 56 (2014) 309 – 316

Physics Procedia

8th International Conference on Photonic Technologies LANE 2014

Bioceramic 3D implants produced by laser assisted additive manufacturing

Fernando Lusquiños[a], Jesús del Val[a], Felipe Arias-González[a], Rafael Comesaña[b], Félix Quintero[a], Antonio Riveiro[a], Mohamed Boutinguiza[a], Julian R. Jones[c], Robert G. Hill[d], Juan Pou[a,*]

[a]*Applied Physics Dpt., Universidade de Vigo, EEI, Lagoas-Marcosende, E-36310, Vigo, SPAIN*
[b]*Materials Engineering, Applied Mech. and Construction Dpt., Universidade de Vigo, EEI Vigo, SPAIN*
[c]*Department of Materials, Imperial College London, South Kensington Campus, London SW7 2AZ, UK*
[d]*Barts and the London, Unit of Dental and Physical Sciences, Mile End Road, London E1 4NS, UK*

Abstract

Cranial defect restoration requires a suitable implant capable to fulfill protective and aesthetic functions, such as polymeric and metallic implants. Nevertheless, the former materials cannot provide osteointegration of the implant within the host bone nor implant resorption, which is also required in pediatric orthopedics for normal patient growth. Resorbable and osteoconductive bioceramics are employed, such as silicate bioactive glasses. Nevertheless, manufacturing based on conventional casting in graphite moulds is not effective for warped shape implants suitable for patient tailored treatments.
In this work, we analyze the application of rapid prototyping based on laser cladding to manufacture bioactive glass implants for low load bearing bone restoration. This laser-assisted additive technique is capable to produce three-dimensional geometries tailored to patient, with reduced fabrication time and implant composition modification. The obtained samples were characterized; the relationships between the processing conditions and the measured features were studied, in addition to the biological behavior analysis.

Peer-review under responsibility of the Bayerisches Laserzentrum GmbH

Keywords: Laser additive manufacturing; laser cladding; bioceramics; bone regeneration

* Corresponding author. Tel.: +34-986812216 .
E-mail address: jpou@uvigo.es

Peer-review under responsibility of the Bayerisches Laserzentrum GmbH
doi:10.1016/j.phpro.2014.08.176

1. Introduction

The materials employed for regenerative bone treatment must exhibit a non-cytotoxic behavior, in addition to a supplementary ability to boost the growth and recovery of lost bone. When the aimed biocompatibility and bioactivity is combined by high mechanical resistance, the challenge is faced by a metal-based implant, and the non-cytotoxic behaviour is achieved by blocking the release of metallic ions. High corrosion resistance titanium alloys are frequently employed; *Long et al.* (1998), *Geetha et al.* (2009). The bioactive property in such high load bearing implants is externally conferred by a surface treatment *Liu et al.* (2004). In applications where the high mechanical resistance is not an essential requirement, such as treatments after trauma or surgical resection of low load-bearing bone, the main goal is the material bioactivity. Bioceramics based on silicate bioactive glass and calcium phosphate are frequently employed for this regenerative treatment approach due to a high osteoconductivity and bone bonding ability *Hench and Wilson* (1993). In order to fulfil the complete function, the ceramic implant geometry must resemble the original bone, supporting and guiding the growth of the surrounding healthy bone. In craniofacial applications, the modern observation techniques employed for diagnostics are able to provide very accurate layered computer models of the implant desired geometry. Nevertheless, the patient-tailored implant manufacture presents problems when conventional techniques are employed to shape ceramic materials. A number of alternative techniques have been introduced, but a definitive technique has not been established; *Clupper et al*. (2001); *Chua et al.* (2004); *Bertrand et al.* (2007). The brittleness and thermal shock susceptibility of bioactive ceramics is a major drawback, as well as the requirement of supplementary processing stages, and the introduction of toxic intermediate additives during manufacturing.

The objective of this study is the analysis of the capabilities of rapid prototyping based on laser cladding to create fully bioceramic implants from bioactive glass precursors, and the assessment of the ideal precursor powder for the technique. Special attention is paid to the thermal evolution of the material during processing and the associated implant structure and bioactive properties, in order to identify the outcome of processing parameters. The technique of laser cladding with powder feeding is a process progressively considered for research in the biomaterials field: the surface treatment approach conducted to calcium phosphate and bioactive glass coatings on Ti6Al4V alloy [*Lusquiños et al.* (2001, 2003, 2005); *Comesaña et al.* (2010); also for processing three-dimensional calcium phosphate parts and bioactive glass; *Comesaña et al.* (2011). In the rapid prototyping based on laser cladding technique, microparticles of precursor material are injected as a carrier gas-powder stream on a disposable substrate, which is moving across this powder flow and the laser beam. A stationary high power laser radiation is directed to the surface of the substrate. The laser beam heats up the precursor material stream and a molten pool is initially created on the substrate where the particles impinge. Solidification takes place when the laser beam goes away from the molten pool. The first ceramic material strip is solidified over the disposable substrate. The following material strips are sequentially deposited overlaying the previous strip. Thus, a layered part is built when superposing several strips.

From the irradiance and material-radiation interaction time applied by the technique, the Rapid prototyping based on laser cladding can be identified as a thermal technique. When a thermal technique is employed to transform glass, the specific glass thermal points and its working range are important properties. In general, in thermal working processes the glass transition point denotes the temperature at which viscous flow starts and it is possible to shape the material. Additionally, the crystallization temperature denotes the onset of structural modifications conducting to the origination of a crystalline phase that deteriorates the material workability. For most industrial applications, the glass composition is changed to improve the thermal shock resistance and to increase the glass working range (temperature interval where the viscosity allows shaping the material without undesired structural changes). Extensive research effort has been directed to obtain correlations between the oxides content of the glass and its thermal properties. Moreover, other important requirements such as the coefficient of thermal expansion or the glass appearance must be achieved for a particular application. As a consequence, small variations in the composition of the glass lead to important changes in the glass suitability for the pair specific manufacturing technique and specific glass part function.

When the bone regeneration function is the objective, the glass osteoconductivity and osteoinductivity is a primary goal, and must be maximized. Such enhanced bioactivity is, nevertheless, determined by the glass composition and the obtained thermal shock resistance and working range for higher bioactivity compositions are

considerable smaller than those desired. The bioglass 45S5® is referred as the glass with higher bioactivity level, showing high reactivity and osteoconductive behavior. However, its elevated crystallization tendency is reported by *Artila et al.* (2008) to difficult both shaping and densification. Alternative glass compositions have been proposed, with the aim of preserving the amorphous structure during processing and attaining a still high osteoconductive implant. But few of them achieved the compromise between working range and elevated bioactivity. Among the alternative compositions, the S520 bioactive glass and the 13-93 bioactive glass stand out due to their compromise between working range for thermal processes and osteoconductivity level; *Clupper et al*. (2001); Fu et al. (2008). On the other side, some works state that glass-ceramics derived from 45S5 bioactive glass maintain the biological apatite precipitation ability in SBF (Simulated Body Fluid); therefore, an eventual devitrified implant obtained from this well-known glass composition would be still interesting from the bioactivity point of view; *Peitl et al.* (1996); *Clupper et al.* (2002).

2. Materials

Bioactive silicate glass compositions used in this work and respective precursor mixtures are found in works by *Comesaña et al.* (2010, 2011). The bioactive glass with composition equivalent to 45S5 Bioglass® and S520 were obtained from the decarbonation and melting of the mixture and subsequent refinement at 1400 ºC for 1 hour in a Pt crucible. All glass melts were rapidly quenched in water and subsequently dried. The obtained glass frits were ground by means of agate mill and sieved to a particle size between 60 µm and 150 µm. Glass powder with particle size below 45 µm was heated from room temperature to 1100 ºC, at a heating rate of 20º/min in a nitrogen atmosphere. The approximate glass transition temperature (Tg) are extracted from differential scanning calorimetry analysis of the glasses, being 490 and 560 ºC for S520 and 45S5, respectively. Similarly, the observed crystallization peak temperatures (Tp) for this particular heating rate are 675 and 700 ºC for S520 and 45S5, respectively. More extensive thermal analysis and temperature characteristic points of both glass compositions can be consulted in the previously mentioned work. Processed samples obtained from 45S5 bioactive glass particles will be denominated LC45, while those obtained from S520 bioactive glass processing will be denominated LC52. The S520 bioactive glass lower crystallization tendency and smooth behaviour around softening point, along with an acceptable bioactive behaviour, makes this glass composition an interesting compromise for laser thermal induced processes.

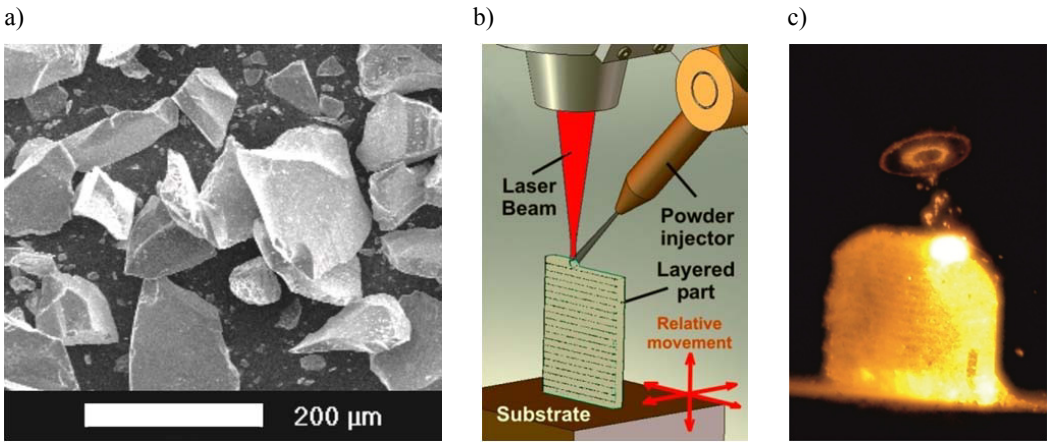

Fig. 1. (a) Scanning electron micrograph showing the size and morphology of the bioactive glass particles employed as precursor material; (b) diagram of the rapid prototyping based on laser cladding technique; (c) layered glass-derived bioceramic at high temperature during processing.

3. Methods

The laser source employed was a CO_2 laser (Rofin SCx10) emitting at the fundamental wavelength of $\lambda = 10.6$ μm and a maximum power of 140 W. The laser beam polarization is converted from linear to circular by means of a λ/4 mirror in order to avoid directional heterogeneity during processing. The radiation was coupled to the working station via expanding and collimating optics, while the laser beam was focused using a lens with 190.5 mm of focal length. The bioactive glass precursor powders were injected in the interaction zone by means of argon conveying streams and gas-solid injectors coupled to a hopper. The configuration of the gas-solid injector consisted in an axial nozzle and the vertical hopper on the side. The substrate temperature was maintained at 225 ºC to avoid sample cracking. A bioactive glass part was created by a three-dimensional relative movement between the working head and the substrate. A value of 20 mg/s was kept constant for the bioactive glass mass flow with volumetric flow values of protective inert gas covering from 1.8 to 8.0 l/min. The profile of the processed part after each deposited layer was monitored by means of a CCD camera in order to keep invariable the geometrical configuration between the laser beam, the powder stream and the processed part.

In order to observe the molten pool evolution during processing, the process was monitored by means of a Photron Fastcam 1024 high speed video camera, operating with 1.5 μs frame exposition time and a maximum sampling frequency of 1500 frames/s. The direction of observation was perpendicular to the sample side and a 200 W halogen light was oppositely placed for background illumination. The absorbed energy and temperature reached by the glass particles just before impinging on the molten pool was calculated from the powder stream-laser beam geometrical configuration, the powder size data and the calorimetry data. In addition, the observation of the largest particles shape evolution when trapped by the molten pool allowed to estimate when is reached the glass softening temperature. The radiation emitted by the surface of the deposited material was recorded by means of a Maurer KTR 1475 pyrometer to estimate and compare the cooling rate produced by different process settings. The temperature decrease was recorded at an intermediate point of the surface and was averaged from 10 processed samples. In order to avoid interference with background illumination, pyrometer measuring was performed separately to high speed video recording.

In order to study the obtained implants microstructure, crystallinity was analyzed by means of a PANalytical X'Pert Pro X-ray diffractometer, using monochromated Cu-Kα radiation ($\lambda = 1.54$ Å). Diffractograms were obtained directly from the sample side surface and from the complete samples after milling to a particle size below 40 μm. The microstructure and local elemental composition was examined via scanning electron microscopy (SEM Philips XL-30) and an energy dispersive X-ray spectroscope coupled to the microscope (EDS EDAX PV9760). Fourier transform infrared spectra of the overall samples were acquired by a Thermo Nicolet 6700 spectrometer. To examine structural differences within the sample a Continuum IR microscope coupled to the spectrometer was used to collect the reflectance FTIR spectra between 650 and 1200 cm-1, scanning 100 x 100 μm2 areas along the sample surface and cross section.

In order to study dissolving rates in simulated physiological fluid, the processed implants were placed in separate plastic containers with 150 mL of 0.05 M Tris-HCl buffer (Tris(hydroxyl)methyl-aminomethane-HCl), pH = 7.4 at 36.5ºC. Immersed samples and solution were kept at 36.5 ºC under stirring. Precursor 45S5 bioactive glass bulk samples with the same dimensions as the laser processed samples were tested for comparison purposes. Spectroscopic elemental analyses were performed with inductively coupled plasma optical emission spectroscopy (Perkin Elmer Optima 4300 DV). Calibration for Ca, Si, P, Na and K analysis were performed with 10 mg/L standards with RSD values below 2.0 %.

4. Results and discussion

4.1. Processed implants structure and process optimization

The analysis of the bioceramic implant composition after processing 45S5 and S520 bioactive glasses revealed the preservation of composition, in terms of elemental composition correspondence to precursor glasses and homogeneity of composition along the processed part. The precursor glass particles are subjected to a thermal cycle that starts during the injection within the carrier gas-powder stream. The CO_2 laser radiation is highly absorbed by

the silica chains of the glass structure, and the particles are preheated. Nevertheless, the particle temperature does not reach the glass transition point during flight due to the high injection speed and short irradiation time. The high speed video observations revealed that the glass particles start to soften and melt after arrival to the molten pool. Once the particles are incorporated to the molten pool, heating by means of conduction and laser absorbance reaches the glass melting temperature in few milliseconds, thus there is no time for nucleation of crystal growth. As a consequence the structure of the processed bioceramic implant is governed by the cooling from the molten pool temperature. The fact that the material is not merely sintered, as in other thermal based freeform techniques, is a special feature of the rapid prototyping based on laser cladding when processing bioceramics. Moreover, volatilization of the present chemical species in thermal processing starts at 1050 ºC and growths with time and temperature. With this technique, the glass is exposed to such high temperatures for very short times, and volatilization is minimized in comparison with weight loss produced by other thermal processes that require extended times at high temperature.

The registration of the temperature during cooling revealed a similar thermal cycle and allowed to estimate cooling rates for both bioactive glasses. Due to the use of identical processing parameters, the thermal input was the same for both glasses. As the calorific capacity of the two glasses is very similar, the experimental temperature measurements are in well agreement with the expected behaviour. When the laser beam moves along the processed part, the deposited glass is observed to rapidly cool until 900 ºC with an estimated cooling rate of 450 ºC/min. Following, the temperature decays linearly until 600 ºC; in this interval the average cooling rates were around 80 ºC/min. On the contrary, despite the almost identical thermal cycle experienced by the two glasses, the XRD analysis provided notably different results. Devitrification was observed in laser processed samples surface for both glass compositions (see Fig. 2.a and Fig. 2.b); however, further observation indicates that crystallization in samples obtained from 45S5 bioactive glass is not limited to the surface and extends across the sample inner material. In addition, differences in peak intensity between surface and crushed sample diffractograms reflect crystal preferential growth produced at surface. On the other side, the samples obtained by feeding S520 bioactive glass exhibited a lower tendency to crystallization. The crystalline phase detected in the processed samples was the silicate $Na_2Ca_2Si_3O_9$, in agreement with the reported XRD pattern and crystal phase grown in 45S5 bioactive glass subjected to thermal treatment; *Arstila et al.* (2008). Sodium-calcium silicates close to $Na_2Ca_2Si_3O_9$ can be present as solid solution; therefore, composition differences can exist within crystal aggregates. The similarity between the crystal aggregate composition and that of the stable phase, found in the processed samples, indicates an advanced stage of crystallization for 45S5 derived samples. In these conditions, the employed glass working window becomes important to obtain vitreous implants. In addition, if the manufacture of moderate size implants is aimed, the thermal working window must cover thermal conditions that progressively deviate along the implant gowth.

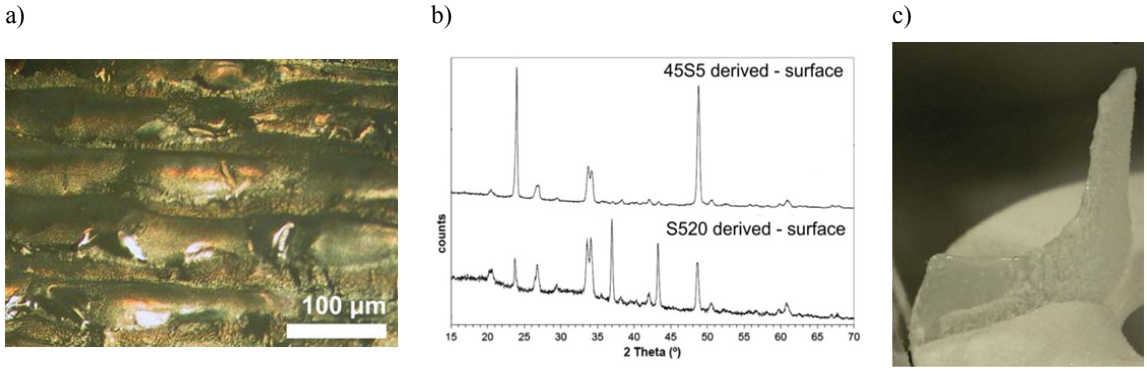

Fig. 2. (a) Optical micrograph of the glass derived bioceramic surface showing the superimposed layers; (b) X-ray diffractograms acquired from the surface of the samples obtained from 45S5 and S520 bioactive precursors; (c) Layered bioceramic implants produced by rapid prototyping based on laser cladding of 45S5 bioactive glass; the part is generated from a three-dimensional CAD model of a cranial bone defect.

In order to obtain sound bioceramic implants form 45S5 and S520 bioactive glass precursors, the optical power, the protective gas and the glass particles mass flow were modified during tests. Moreover, the substrate was preheated to preclude cracking due to thermal shock in the initial deposited layers. Low values for the protective gas flow were required to avoid cracking at any stage of the process, as this gas flow modifies the convection around the working zone, with additional implications on the obtained glass structure. Optimum values of processing parameters to obtain sound samples were: laser optical power 33 W, scanning speed 5 mm/s, mass flow 20 mg/s, protective gas flow 2.0 l/min. Figure 2.c shows a 45S5 derived bioceramic sample obtained under optimized conditions. The sample was generated from a three-dimensional CAD model of a cranial defect; the working head trajectories were calculated through stereolithography file conversion (stl file conversion).

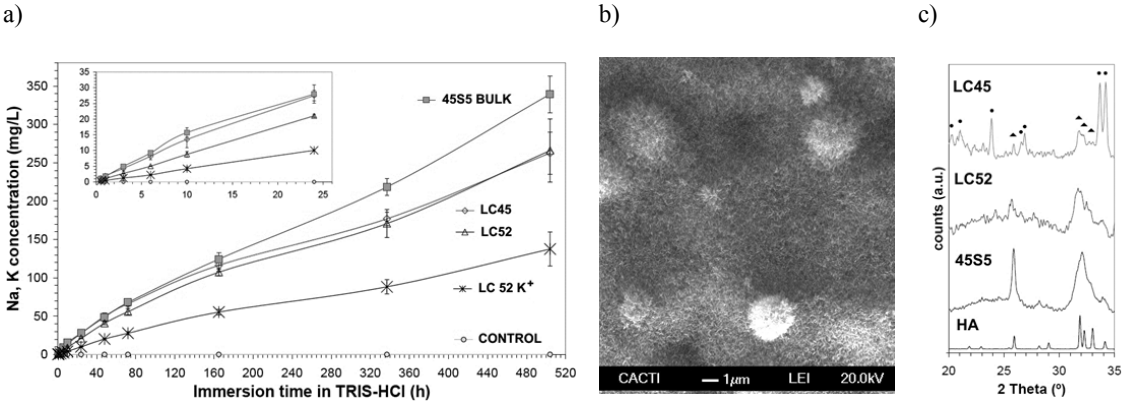

Fig. 3. (a) Sodium and Potassium ion release profile of the glass derived implants and the reference 45S5 bioglass during immersion in Tris-HCl buffer under body conditions; (b) SEM micrograph of the immersed sample surface showing precipitated apatite; (c) X-ray diffractograms of the immersed samples after 3 weeks and pattern of the biological apatite.

4.2. Ion release profiles under simulated body conditions

In order to predict the expected bioactivity, the samples obtained below optimized processing conditions were subjected to immersion in Tris-HCl buffer at body pH and temperature. The Figure 3.a) displays the ICP results for sodium and potassium ion release within 3 weeks. 45S5 as cast glass was employed as control. For LC52 samples obtained from S520 bioactive glass particles, similar behaviour to precursor glass is observed. On the contrary, dissolution differences between LC45 samples and 45S5 reference are attributed to wide crystallization. Further ICP results of concentration change in Tris-HCl solution after sample immersion indicates that the release of Ca^{2+} ions of LC45 samples follows a similar pattern than the one observed for 45S5 bioactive glass cast samples. Measured Ca^{2+} concentration values for LC52 samples were lower than those observed for 45S5 bioactive glass and LC45 samples; due to lower CaO content in the glass and higher network connectivity of S520 bioactive glass (due to higher silica content the glass structural network is more connected, leading to higher durability). Observed concentrations are in good agreement with the reported dissolution behaviour of 45S5 bioactive glass by *Peitl et al.* (2001).

Apatite precipitation indications were observed in the maximum concentration values of P produced first for bulk 45S5 bioactive glass control samples at 22 h; then at 63 and 70 h for LC45 and LC52 samples, respectively. Precipitated apatite in samples after 3 weeks is corroborated by SEM (see Fig. 3.b). In addition, the XRD analysis of the immersed surfaces allow to appreciate that the peaks of crystalline silicate disappear from LC52 samples, while are still present in LC45 diffractograms (see Fig. 3.c). Devitrification of bioactive glass 45S5 subjected to thermal processing has been observed to slow the rate of apatite precipitation under body conditions; although extensively crystallized glass-ceramics still show similar bioactivity to that of the parent glasses. Thus, it can be affirmed that the S520 bioactive glass is more appropriate to be processed by rapid prototyping based on laser cladding.

5. Conclusions

The application of laser cladding to three-dimensional processing of bioactive glass revealed full density of produced samples by cooling from melting temperature in the laser-material interaction area. Injected glass particles temperature increases at very high rate, being the obtained microstructure governed by the cooling history. The cooling rate of the deposited material can be adjusted by processing parameters modification; hence, cracking is avoided over the built three-dimensional implant.

No species volatilization is produced and chemical composition of bioactive glass is maintained after the process. Structural modifications consist of surface crystallization, which exhibit reduced reach in S520 bioactive glass samples, but extends over the whole volume in glass-ceramic samples derived from 45S5 bioactive glass.

Processed samples show ion release profiles in Tris-HCl buffer that are comparable to these produced by the precursor bioactive glasses. Ability of apatite formation in SBF is observed, with similar reaction rates than precursor glasses. The obtained results states that initial material bioactive properties are generally unaffected by processing by rapid prototyping based on laser cladding.

Acknowledgements

This work was partially funded by the European Union Cross-border cooperation programme 2007-2013 (Project 0330_IBEROMARE_1_P), the Spanish Government and FEDER (CICYT MAT2006-10481), FPU AP2006-03500 grant and by Xunta de Galicia (IN845B-2010/082).

References

Long, M., Rack, H.J., 1998. Titanium alloys in total joint replacement - A materials science perspective. Biomaterials, 19, 1621-1639.

Geetha, M., Singh, A.K., Asokamani, R., Gogia, A.K., 2009. Ti based biomaterials, the ultimate choice for orthopaedic implants - A review Progress in Materials Science, 54, 397-425.

Liu, X., Chu, P.K., Ding, C., 2004. Surface modification of titanium, titanium alloys, and related materials for biomedical applications Materials Science and Engineering R: Reports, 47 (3-4), pp. 49-121.

Hench, L.L., Wilson, J., 1993. An introduction to bioceramics. Singapore: World Scientific.

Clupper, D.C., Mecholsky, J.J., LaTorre, G.P., Greenspan, D.C., 2001. Sintering temperature effects on the in vitro bioactive response of tape cast and sintered bioactive glass-ceramic in Tris buffer. J Biomed Mater Ress;57;532-40.

Chua, C.K., Leong, K.F., Tan, K.H., Wiria, F.E., Cheah, C.M., 2004. Development of tissue scaffolds using selective laser sintering of polyvinyl alcohol/hydroxyapatite biocomposite for craniofacial and joint defects. J Mater Sci: Mater Med, 15, 1113-21.

Bertrand, Ph., Bayle. F., Smurov, I., 2007. Yttria-zirconia components manufacturing for biomedical applications by SLS technology, in Proceedings of the International Congress on Applications of Lasers & Electro-Optics, Orlando, USA,192-5.

Lusquiños, F., Pou, J., Arias, J.L., Boutinguiza, M., Pérez-Amor, M., León, B., Driessens , F.C.M., 2001. Production of calcium phosphate coatings on Ti6Al4V obtained by Nd:yttrium-aluminum-garnet laser cladding. J Appl Phys 90, 4231-6.

Lusquiños, F, De Carlos, A, Pou, J, Arias, JL, Boutinguiza, M, León, B, Pérez-Amor, M, Driessens, FCM, Hing, K, Gibson, I, Best, S, Bonfield, W., 2003. Calcium phosphate coatings obtained by Nd:YAG laser cladding: physico-chemical and biological properties. J Biomed Mater Res;64A: 630 637.

Lusquiños, F., Pou, J., Boutinguiza, M., Quintero, F., Soto, R., León, B., Pérez-Amor, M., 2005. Main characteristics of calcium phosphate coatings obtained by laser cladding. Applied Surface Science 247, 486-492.

Comesaña, R., Quintero, F., Lusquiños, F., Pascual, M.J., Boutinguiza, M., Durán, A., Pou, J., 2010. Laser cladding of bioactive glass coatings. Acta Biomaterialia 6, 953-961.

Comesaña, R., Lusquiños, F., del Val, J., Malot, T., López-Álvarez, M., Riveiro, A., Quintero, F., Boutinguiza, M., Aubry, P., De Carlos, A., Pou, J., 2011. Calcium phosphate grafts produced by rapid prototyping based on laser cladding. Journal of the European Ceramic Society 31, 29-41.

Comesaña, R., Lusquiños, F., del Val, J., López-Álvarez, M., Quintero, F., Riveiro, A., Boutinguiza, M., De Carlos, A., Jones, JR., Hill, RG., Pou, J., 2011. Three-dimensional bioactive glass implants fabricated by rapid prototyping based on CO2 laser cladding. Acta Biomaterialia 7, 3476-3487.

Arstila, H., Hupa, L., Karlsson, K.H., Hupa, M., 2008. Influence of heat treatment on crystallization of bioactive glasses. J Non-Cryst Sol 354, 722-728.

Fu, Q., Rahaman, M.N., Bal, B.S., Brown, R.F., Day, D.E., 2008. Mechanical and in vitro performance of 13-93 bioactive glass scaffolds prepared by a polymer foam replication technique. Acta Biomaterialia 4, 1854-64.

Peitl, O., LaTorre, G.P., Hench, L.L., 1996. Effect of crystallization on apatite-layer formation of bioactive glass 45S5. J Biomed Mater Res Part A 30, 509-514.

Clupper, D.C., Mecholsky, J.J., LaTorre, G.P., Greenspan, D.C., 2002. Bioactivity of tape cast and sintered bioactive glass-ceramic in simulated body fluid. Biomaterials 23, 2599-606.

Peitl, O., Zanotto, E.D., Hench, L.L., 2001. Highly bioactive P_2O_5-Na_2O-CaO-SiO_2 glass ceramics. J Non Cryst Sol 292, 115-126.